Article

Knockdown of the ADHD Candidate Gene *Diras2* in Murine Hippocampal Primary Cells

Journal of Attention Disorders
2021, Vol. 25(4) 572–583

DOI: 10.1177/1087054718822129
journals.sagepub.com/home/jad
SAGE

Lena Grünewald[1], Andreas G. Chiocchetti[1], Heike Weber[1,2], Claus-Jürgen Scholz[3], Christoph Schartner[2,4], Florian Freudenberg[1], and Andreas Reif[1]

Abstract

Objective: The *DIRAS2* gene is associated with ADHD, but its function is largely unknown. Thus, we aimed to explore the genes and molecular pathways affected by *DIRAS2*. **Method:** Using short hairpin RNAs, we downregulated *Diras2* in murine hippocampal primary cells. Gene expression was analyzed by microarray and affected pathways were identified. We used quantitative real-time polymerase chain reaction (qPCR) to confirm expression changes and analyzed enrichment of differentially expressed genes in an ADHD GWAS (genome-wide association studies) sample. **Results:** *Diras2* knockdown altered expression of 1,612 genes, which were enriched for biological processes involved in neurodevelopment. Expression changes were confirmed for 33 out of 88 selected genes. These 33 genes showed significant enrichment in ADHD patients in a gene-set-based analysis. **Conclusion:** Our findings show that *Diras2* affects numerous genes and thus molecular pathways that are relevant for neurodevelopmental processes. These findings may further support the hypothesis that *DIRAS2* is linked to etiological processes underlying ADHD. *(J. of Att. Dis. 2021; 25(4) 572-583)*

Keywords
expression studies, neurodevelopmental disorders; adeno-associated virus; viral gene transfer; RNAi

Introduction

ADHD is a neurodevelopmental disorder emerging in childhood but with a high persistence into adulthood (Faraone et al., 2015; Matthews, Nigg, & Fair, 2014; Thapar & Cooper, 2016). Individuals suffering from ADHD show, depending on the presentation of the disorder, an increase in impulsivity and hyperactivity and/or in inattention (Epstein & Loren, 2013; Faraone et al., 2015). ADHD cumulates within individual families, marking the strong genetic component of this disorder. Twin studies revealed a heritability of ADHD of almost 80% (Faraone et al., 2005). Like other psychiatric disorders, ADHD is genetically complex and several genetic variations and environmental factors interact in the pathophysiology of this disease (Faraone et al., 2015; Faraone et al., 2005; Nigg, Nikolas, & Burt, 2010).

To identify chromosomal regions that harbor susceptibility genes for ADHD, numerous genome-wide association studies (GWAS) and whole genome linkage studies were conducted within the last years (e.g., Demontis et al., 2017; Lesch et al., 2008; Martin et al., 2017; Neale et al., 2010). The chromosome 9q22 locus emerged in two independent linkage studies (Asherson et al., 2008; Romanos et al., 2008) and one GWAS (Lesch et al., 2008) on ADHD. This region comprises the locus of the member of the distinct subgroup of Ras kinases 2 (*DIRAS2*) gene, which is predominantly expressed in the brain (Kontani et al., 2002).

Although in more recent studies no genome-wide association of *DIRAS2* with ADHD was found (Demontis et al., 2017; Martin et al., 2017), significant association of *DIRAS2* with ADHD was confirmed in a gene-based study (Reif et al., 2011). Genotyping of 14 representative single-nucleotide polymorphisms (SNPs) located within or near the *DIRAS2* gene revealed association of the promoter SNP rs1412005 with ADHD. The association was initially identified in a German adult ADHD case-control sample and has successfully been replicated in a family based ADHD sample. Finally, meta-analysis across four adult ADHD patient cohorts from different countries also confirmed association of the haplotype block with the disorder (Reif et al., 2011).

[1]University Hospital, Goethe University Frankfurt, Germany
[2]University Hospital Würzburg, Germany
[3]University of Würzburg, Germany
[4]University of California, San Francisco, USA

Corresponding Author:
Lena Grünewald, Department of Psychiatry, Psychosomatic Medicine and Psychotherapy, University Hospital, Goethe University Frankfurt, Heinrich-Hoffmann-Str. 10, 60528 Frankfurt, Germany.
Email: lena.gruenewald@kgu.de

The risk allele of the *DIRAS2* promoter SNP causes an increased gene expression in a luciferase promoter assay. In addition, children with ADHD carrying the risk allele show an altered NoGo anteriorization in EEG during a Go/NoGo task indicating an altered response inhibition, which is a putative endophenotype of ADHD (Grünewald et al., 2016).

The *DIRAS2* gene is coding for a small Ras kinase with mostly unknown function. Although related in sequence, Di-Ras proteins (Di-Ras1 and Di-Ras2) differ in their biochemical and functional properties from other Ras family members. Like most Ras kinases, they have a highly conserved GTP-binding domain, an effector domain and a membrane-localizing motif at the carboxyl terminus. In contrast to other Ras kinases, Di-Ras1 and 2 carry amino acid substitutions at positions critical for GTP hydrolysis. This biochemical property fits to the finding that in living cells Di-Ras proteins are mainly found in GTP-bound form (Kontani et al., 2002).

Here, we aimed to identify the molecular pathways affected by *DIRAS2* by removing this gene from its molecular network. To this end, we conducted short hairpin RNA (shRNA)-mediated *Diras2* knockdown in murine hippocampal primary cells using recombinant adeno-associated virus (rAAV)-mediated gene transfer. We show that *Diras2* affects expression of numerous genes, thus modulating several pathways, many of which are associated with neurodevelopment. Interestingly, we found that a number of genes affected by *Diras2* are also enriched in genes previously associated with ADHD.

Materials and Methods

Murine Hippocampal Primary Cell Culture

Wild-type C57BL/6J mice, housed in a colony room under controlled ambient conditions (21 ± 1°C, 55 ± 5% humidity), with lights on between 6:00 a.m. and 6:00 p.m. and *ad libitum* access to food and water were used for the primary cell cultures. Mouse maintenance and breeding were performed by experienced personnel, and mice were treated according to the Directive of the European Communities Council of November 24, 1986 (86/609/EEC) and German animal welfare laws (TierSchG and TSchV). Dams were killed by trained personnel, and hippocampi were dissected from mouse embryos at embryonic day 18 (E18). The hippocampi of 1-2 litters (~5-8 embryos/litter) were pooled and the tissue was digested in 0.05% Trypsin/EDTA (ethylenediaminetetraacetic acid) at 37°C for 5 min. To separate the cells, hippocampi were triturated by pipetting up and down using a fire-polished glass Pasteur pipette. Cells were plated at a density of 3×10^4 cells/cm^2 in poly-D-lysine-coated six-well plates. Cells were cultured for 7 days in Neurobasal media with B27 supplement (Gibco) at 37°C prior to rAAV infection.

Generation of shRNA-Expressing pAAV Constructs

For the expression of shRNAs, we generated a novel AAV plasmid (pAAV) named pAAV-U6-hSyn::mCherry.3xFLAG-WPRE expressing shRNAs under the control of the mouse U6 promotor and coexpressing the red monomeric fluorescent molecule mCherry tagged with the FLAG epitope and the mRNA stabilizing Woodchuck Hepatitis Virus Posttranscriptional Regulatory Element (WPRE) under the human *Synapsin 1* promoter (hSyn). To this end, a linker sequence with MluI overhangs containing BstBI, BspQI, and SacI restriction sites was obtained by annealing two oligonucleotides, MluI-Linker(+) and MluI-Linker(–); for sequences see Supplemental Table 1. This linker was inserted into the MluI site of pAAV-hSyn::mCherry.3xFLAG-WPRE (Candemir et al., 2016) using T4 ligase (Fermentas) resulting in pAAV-Linker-hSyn::mCherry.3xFLAG-WPRE. Adapting the cloning strategy used by J.-Y. Yu, DeRuiter, and Turner (2002), the murine U6 promoter was amplified by PCR on mouse genomic DNA using the primers Mm_U6_BstBI_F and Mm_U6_SacI_R (Supplemental Table 1). The U6 promoter was inserted into pAAV-Linker-hSyn::mCherry.3xFLAG-WPRE at the BstBI and SacI sites resulting in pAAV-U6-hSyn::mCherry.3xFLAG-WPRE (Figure 1A).

The insertion site of the novel pAAV-U6-hSyn ::mCherry.3xFLAG-WPRE vector was constructed similar to the vector created by Naughton, Han, and Gu (2011). Thus, this vector system allows easy cloning of the target-specific shRNAs into the open reading frame of the U6 promoter using a single restriction enzyme (i.e., BspQI). Complementary oligonucleotides coding for the shRNA sequences specific for *Diras2* or containing a scrambled sequence as negative control (Supplemental Table 1) were annealed and ligated with the vector construct linearized by BspQI treatment. The annealed oligonucleotides (Figure 1B) contained a 5′-TTG overhang at the 5′ end, which includes the transcriptional start (G), thus requiring the target recognition sequence to start with a G (compare with J.-Y. Yu et al., 2002), and a AAA-5′ overhang at the 3′ end. Moreover, a T was added to the 3′ end of each (+) oligonucleotide to complement the termination signal to contain 5xT. The loop sequence TTCAAGAGA used for all shRNAs was based on that used by Brummelkamp, Bernards, and Agami (2002). Expression of the cloned constructs is predicted to result in the formation of shRNAs targeting *Diras2* or a scrambled sequence (Figure 1C). All constructs were verified by Sanger sequencing (Eurofins Genomics, Ebersberg, Germany). All plasmids are made available through Addgene (https://www.addgene.org/browse/article/28197078/).

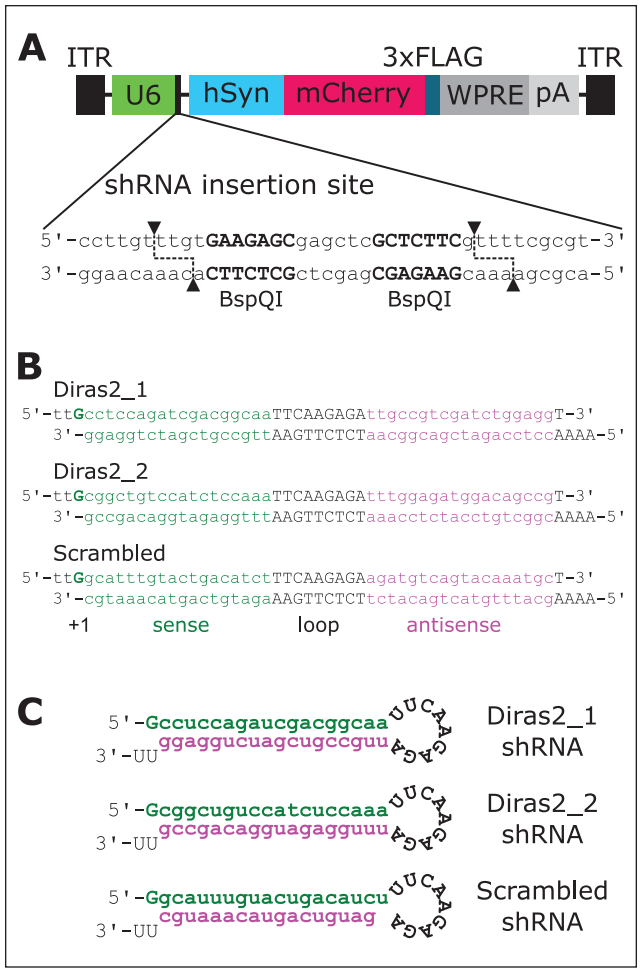

Figure 1. Schematic illustration of the shRNA cloning strategy.
Note. (A) Schematic of the pAAV-U6-hSyn::mCherry.3xFLAG-WPRE vector created for shRNA-mediated knockdown. The murine U6 promoter is followed by an shRNA insertion site containing two BspQI sites (recognition sites shown in bold font, cleavage sites indicated by the arrowheads and dashed lines). Digestion by BspQI digestion leaves an AAC-5′ overhang on the 5′ end and a 5′-TTT overhang on the 3′ end. (B) Sense(+) and antisense(–) oligonucleotides coding for the target and loop sequences are annealed leaving a 5′-TTG overhang at the 5′ end and an AAA-5′ overhang at the 3′ end, thus allowing sticky-end insertion into pAAV-U6-hSyn::mCherry.3xFLAG-WPRE linearized by BspQI. (C) Schematic representation of the predicted conformation of the resulting shRNA. ITR = inverted terminal repeat; U6 = murine U6 promoter; hSyn = human *synapsin I* promoter; WPRE = Woodchuck hepatitis virus posttranscriptional regulatory element; pA = human growth hormone polyadenylation signal; shRNA = short hairpin RNA.

Virus Production, Isolation, and Quantification

Forty-eight hours prior to transfection, AAV-293 clones of HEK-293 cells were seeded in five 145-mm petri dishes at a density of 2×10^5 cells/cm^2. When cells reached 70% to 80% confluency, they were transfected using a reaction mixture containing pRV1 (AAV2; 6.25 µg/plate), pH21 (AAV1; 6.25 µg/plate), pFdelta6 (Ad Helper; 25 µg/plate), one of the pAAV constructs described above (12.5 µg/plate), pEGFP-N3 (5 µg/plate), $CaCl_2$ (150 mM) and HEPES buffered saline (HBS). The medium was replaced after 6 h. Seventy-two hours after transfection, cells were scraped in cold PBS and collected in reaction tubes. Cells were centrifuged at 800× g for 10 min, cell pellets were resuspended and incubated for 1 h at 37°C in a buffer containing 20 mM Tris, 150 mM NaCl (pH 8.0), 0.5% sodium deoxycholate and 50 U/ml Benzonase. After two centrifugations at 3,000× g to remove cell debris, the rAAV was isolated from the supernatant using heparin columns (GE Healthcare). After loading the column with the virus particles and washing with buffers containing 20 mM Tris (pH 8.0) and increasing concentrations of NaCl (100 mM, 200 mM, 300 mM), the virus was eluted using buffers containing 20 mM Tris (pH 8.0) and 400 mM, 450 mM, and 500 mM NaCl. Virus was then concentrated using Amicon Ultra-4 centrifugal filter units (Merck Millipore) and the solution was sterile-filtered using a 0.2 µm Acrodisc syringe filter (Sigma-Aldrich).

For virus quantification, the viral titer was determined using qPCR. As a standard, the AAV plasmid construct was used to generate a dilution series with known concentrations. The diluted plasmid and the solutions containing rAAV in an unknown concentration were used as template for qPCR amplifying the WPRE (see Supplemental Table 1 for primer sequences) using SYBR Select Master Mix (ThermoFisher Scientific). Measurements and analysis were performed with a CFX384 and CFX Manager software (Biorad) with the following conditions: (1) 50°C for 2 min, (2) 95°C for 2 min, (3) 40 cycles of 95°C for 15 s, 60°C for 1 min coterminated by a plate read, (4) 95°C for 10 s, (5) melt curve from 65°C to 95°C in increments of 0.5°C for 5 s coterminated by a plate read.

Infection of Murine Primary Cells and Estimation of Knockdown Efficiencies

To knockdown *Diras2* expression, murine hippocampal primary cells were infected with ~1×10^9 viral particles/well after 7 days in vitro (DIV 7) by adding the virus containing solution directly to the growth medium of the primary cells. After 7 days (i.e., on DIV 14), cells were harvested using 500 µL of RNAprotect Cell Reagent (Qiagen, Hilden, Germany). At DIV 14, primary neurons normally would have developed a complex dendritic pattern and started developing dendritic spines (Kaech & Banker, 2006), which was also observed in our cultures. The cells of three identically treated wells were pooled for RNA isolation. RNA was isolated using the RNeasy Plus Mini Kit (Qiagen, Hilden, Germany) following manufacturer's instructions. RNA concentration was estimated by spectrophotometric measurements using a Nanodrop 1000 (Peqlab, Erlangen, Germany).

Diras2 knockdown was confirmed by qPCR using primers specific to *Diras2* as well as *B2m, Pgk1*, and *Hprt*, which were identified in preliminary experiments as the most stable reference genes under these experimental conditions (for primer sequences, see Supplemental Table 1) and SYBR Select Master Mix (ThermoFisher Scientific) on a CFX384 instrument (Biorad) with the following conditions: (a) 50°C for 2 min, (b) 95°C for 2 min, (3) 40 cycles of 95°C for 15 s, 60°C for 1 min coterminated by a plate read, (4) 95°C for 10 s, (5) melt curve from 65°C to 95°C in increments of 0.5°C for 5 s coterminated by a plate read.

Expression Array

For analyses of gene expression in shRNA Diras2_2 and scrambled shRNA-treated samples, GeneChip Mouse Gene 2.0 ST microarrays (Affymetrix, Santa Clara, CA, USA) were used with the Ambion WT Expression Kit (ThermoFisher Scientific) according to the manufacturer's protocol. RNA quality and concentrations were determined by Bioanalyzer measurement (Agilent technologies, Santa Clara, CA, USA). RNA from three different samples (each pooled from three wells) isolated in experiments conducted on different days were used for the expression analyses of each group. Data were preprocessed with the Expression Console v1.2.1.20 software (Affymetrix); background correction, normalization, and gene-level probeset summary were performed with the "RMA sketch" workflow using default parameter settings. Differentially expressed genes were detected using R software in combination with the *limma* package (linear models for microarray data; Smyth, 2004). Array expression data were quantile normalized and differentially expressed genes were identified using generalized linear regression models including random effects for replicates. Genes were declared as differentially expressed with moderated *t* tests resulting in a false discovery rate < 0.05. In this setting, the largest nominal *p* value of differentially expressed genes was 2.378×10^{-3}. Brain-expressed genes were detected using the tissue expression enrichment analysis function provided by DAVID v6.7 (https://david.ncifcrf.gov/).

GO-term enrichment analysis was performed including all transcripts with a false discovery rate < 0.05 using package topGO (Alexa, Rahnenfuhrer, & Lengauer, 2006) implementing the weigth01 algorithm as previously published (Chiocchetti et al., 2016). In contrast to classical GO-term enrichment analysis, the hierarchical structure of GO-terms (i.e., the dependence of parent and child terms) is accounted in the testing procedure. Thus, correction for multiple testing is performed within analysis.

Weighted gene coexpression network analysis (WGCNA) was performed as published previously (Chiocchetti et al., 2016; Haslinger et al., 2018) using the "WGCNA" package with topGO. We set the network type to unsigned with a soft thresholding power of 14. This resulted in a scale-free network structure (model fit $R^2 > 0.9$). Eigenvalues of coregulated modules were compared between groups using *t* test. Coexpression network analysis first identifies gene groups that are correlated across the individual samples. In contrast to differential gene expression analysis, this allows to identify biological processes rather than individual genes. Positively and negatively associated modules do reflect the GO-term association from the differentially expressed gene list, as up- and downregulated genes can be assumed to be correlated, respectively. However, the WGCNA analysis further allows that subtle correlation within the identified gene groups are accounted for in the enrichment analysis, although they would not be tested significant in the group comparison.

Microarray data have been deposited in MIAME-compliant form at Gene Expression Omnibus (GEO; http://www.ncbi.nlm.nih.gov/geo) under Accession Number: GSE66432.

qPCR Validation

To narrow down the number of assays, the 164 genes that showed a significantly altered expression after *Diras2* knockdown and expressed in the brain were screened for interesting candidates based on gene function, involvement of the gene in relevant pathways and expression patterns by literature and database research. Specifically, the selection was performed by searching PubMed (https://www.ncbi.nlm.nih.gov/pubmed/) for the official gene symbol (possibly including common obsolete gene symbols). Titles and abstracts were scrutinized for their potential relevance and a total of 88 genes were selected based on this search.

To technically validate the results of the arrays, the expression of those selected genes was measured in *Diras2* knockdown caused by the same shRNA as used for the array experiments (Diras2_2; $n = 6$ pools [pooled from three different cell culture wells]; three of these were already used for the microarray experiments), in samples with a *Diras2* knockdown induced by an alternative *Diras2*-shRNA (Diras2_1; $n = 6$ pools) and in negative control samples infected with an rAAV expressing a scrambled shRNA sequence ($n = 5$ pools; three of these were already used for the microarray experiments).

Knockdown and RNA isolation experiments on murine hippocampal primary cells were performed as described above. RNA quantity and quality were assessed by capillary electrophoresis using a FragmentAnalyzer and the Standard Sensitivity RNA Analysis Kit DNF-471 (Advanced Analytical).

The expression of 88 genes, selected as described above, and *Pgk1, Rpl13a*, and *Sdha* (which were identified in preliminary experiments as the most stable reference genes under these experimental conditions) was analyzed in singlets using

a RealTime ready Custom Panel 384 – 96+ with Light Cycler 480 Probes Master on a LightCycler480 (Roche) using the following conditions: (a) 95°C for 10 min, (2) 45 cycles of 95°C for 10 s, 60°C for 30 s, 72°C for 1 s coterminated by a plate read. For data processing and statistical analyses GenEx6 (MultiD) was used. The geNorm algorithm determined *Pkg1* and *Sdha* as the most stably expressed reference genes. Thus, quantities were normalized using *Pgk1* and *Sdha* and are given relative to the sample with the highest Cq value. Relative normalized quantities were log2 scaled. To test for significant differences between groups a one-way analysis of variance (ANOVA) was performed. To estimate the direction of the expression changes and to check if the differences are found between the control group and both knockdown groups, a one-sided Bonferroni post hoc test was performed.

The raw data of these qPCR experiments have been deposited at Mendeley Data (http://dx.doi.org/10.17632/rtsx7zpt4w.1).

Association of Differentially Expressed Genes With ADHD

To examine whether the genes that are differentially expressed following *Diras2* downregulation are associated with ADHD, we performed a gene-based association on summary statistics of the European genome-wide meta-analysis on ADHD (Demontis et al., 2017; n_{cases} = 19,099; $n_{controls}$ = 34,194) by use of MAGMA 1.06 (de Leeuw, Mooij, Heskes, & Posthuma, 2015). Only the genes whose differential expression was confirmed by qPCR were used for this analysis. A total of 7,033,390 valid SNPs were annotated including 5 kb up- and 1.5 kb downstream of 17,786 transcribed gene regions, based on the National Center for Biotechnology Information (NCBI) 37.3 gene definitions. TPI1 (7167) could not be annotated and was, therefore, excluded from further analysis. Annotated SNPs were tested for enrichment in each of the differentially expressed genes using the SNP-wise mean model to generate overall gene *p* values. As reference for LD, the European panel of the 1000 Genomes Phase 3 data (Auton et al., 2015), was used for correction.

To determine whether the *DIRAS2* downstream target gene-set, comprising all differentially expressed genes, is more strongly enriched in ADHD than other genes, an additional competitive gene-set analysis was performed based on the gene-based *p* values generated above.

Results

Downregulation of Diras2 Expression

To investigate the effects of *Diras2* on gene expression, we constructed a novel vector system that allows easy cloning of target-specific shRNAs into an rAAV vector (Figure 1). As *Diras2* is highly expressed in the hippocampus (Grünewald et al., 2018) knockdown was performed in murine hippocampal primary cells. Infection of primary hippocampal cell cultures with an rAAV encoding *Diras2*-specific shRNAs (Diras2_1 and Diras2_2, respectively) resulted in highly significant downregulation of *Diras2* expression when compared with uninfected controls (Diras2_1: 0.042 ± 0.002, $p < .001$; Diras2_2: 0.028 ± 0.011, $p < .001$), whereas infection with an rAAV encoding scrambled shRNA had no significant effect on *Diras2* expression (0.771 ± 0.166, $p < .366$).

Expressional Changes Induced by Diras2 Knock Down

To investigate the effects of *Diras2* knock down on gene expression, we compared genome-wide expression levels in primary hippocampal cell cultures infected with rAAVs encoding shRNA Diras2_2 to those infected with scrambled shRNA expressing rAAVs on microarrays ($n = 3$ for Diras2_2 and scrambled shRNA each). Diras2_2 was chosen for these experiments, as this shRNA gave the highest levels of downregulation of *Diras2*. Of 35,240 transcripts detected by the array experiment, 1,612 showed significant expression differences (855 were upregulated and 757 were downregulated) between the knockdown and the control samples after correction for multiple testing. Of note, downregulation of *Diras2* was confirmed on the microarrays, showing more than 11-fold (log2 fold-change = −3.54) reduction. Of the differentially expressed genes, 376 showed at least twofold changes in their expression levels (189 upregulated, 187 downregulated; Supplemental Figure 1, Supplemental Table 2). Filtering for genes that are predominantly expressed in the brain revealed 164 genes (79 upregulated, 85 downregulated; Supplemental Table 3).

GO-term analysis including all 1,612 differentially expressed transcripts associated the upregulated differentially expressed genes with the negative regulation of signal transduction, protein autoubiquitination and post-Golgi vesicle–mediated transport. Downregulated differentially expressed genes were assigned to the positive regulation of GTPase activity, nonmotile primary cilium assembly and chromatin modification. Genes involved in protein transport and nucleotide-sugar metabolic processes were found to be both up- and downregulated (Figure 2A, Supplemental Table 4).

To further analyze the gene expression network affected by *Diras2* downregulation, we performed WGCNA, which revealed a total of 34 coregulated gene modules. The eigenvalue of two of these gene sets was significantly altered by *Diras2* knockdown. GO-term enrichment showed that the positively regulated module contains genes involved in cell division, protein transport, mitotic nuclear division, the cell

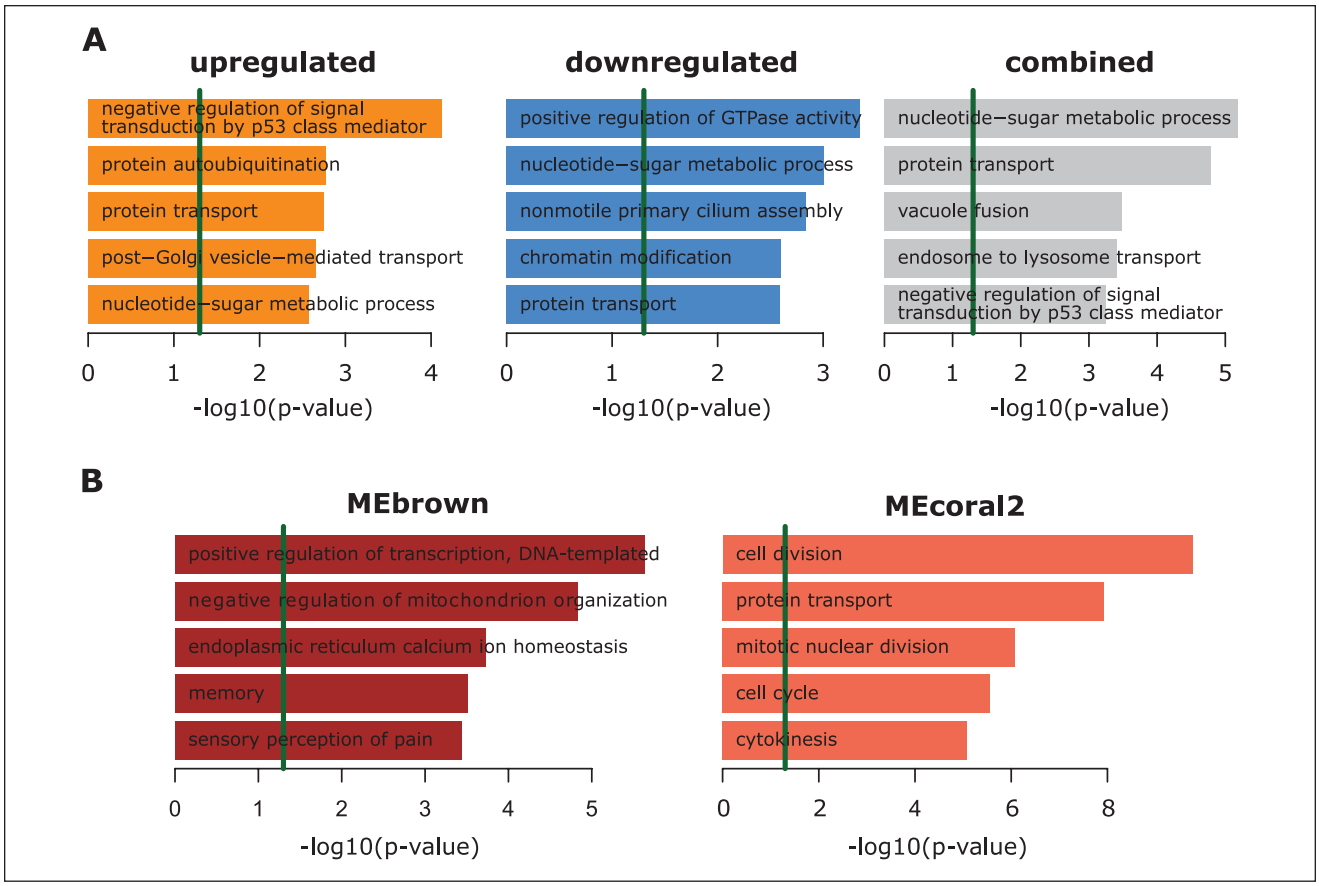

Figure 2. Bioinformatic analysis of gene expression data after shRNA-mediated *Diras2* knockdown. (A) GO-term enrichment of differentially expressed genes. Weighted *p* values of the five most significant terms of significantly upregulated (left), downregulated (middle), and both up- and downregulated combined (right) are shown. Green line marks the weighted $p < .05$ cutoff. A full list of significantly associated GO terms can be found in Supplemental Figure 4. (B) GO-term enrichment analysis of identified network modules from WGCNA. Weighted *p* values of the five most significant terms are shown. Green line marks the weighted $p < .05$ cutoff. A full list can be found in Supplemental Figure 5.

Note. shRNA = short hairpin RNA; WGCNA = weighted gene coexpression network analysis.

cycle and cytokinesis. The negatively regulated module comprises genes that play a role in the positive regulation of transcription, in the negative regulation of mitochondrion organization, the calcium ion homeostasis of the endoplasmatic reticulum, memory and sensory perception of pain (Figure 2B, Supplemental Table 5).

qPCR Validation of Array Experiments

Of the 164 differentially expressed genes that are mainly expressed in the brain, we selected 88 promising candidates based on literature and database search for validation of gene expression by qPCR. Gene expression of these 88 genes was determined in RNA from primary hippocampal cells infected with shRNA Diras2_2 and an alternative shRNA (Diras2_1; $n = 6$ for each of the shRNAs) and compared with RNA from cell cultures infected with scrambled shRNA expressing rAAVs ($n = 5$). For one of the chosen transcripts (*Slk1*), no amplification was achieved. Of the remaining 87 transcripts whose normalized relative quantities were determined, 11 transcripts showed opposite expression changes for both shRNA (i.e., one shRNA resulted in upregulation and the other in downregulation), two showed the opposite direction of regulation than that observed on the microarray and for one gene (*Nos1*) we observed expression changes congruent with those observed on the array, which were, however, not significant. Of the remaining transcripts, 55 showed nominally significantly altered expression levels (i.e., *p* values for both shRNAs were below the uncorrected significance threshold of 0.05). After correction for multiple testing (significance threshold $p \leq .00057$, 33 of these genes showed significant expression changes after downregulation of *Diras2* with both shRNAs and with the same effect direction as observed in the array experiments (Table 1, Supplemental Table 6). Our findings indicated that *Diras2* exerts the strongest effects on *Ankrd34b, Clasp2, Eif2c2, Lnp, Mfsd11, Setd6*, and *Tpi1*, which showed the most significant changes ($p \leq 1 \times 10^{-8}$).

Table 1. Genes That Were Found to Be Significantly Up- or Downregulated in the qPCR Experiment After *Diras2* Knockdown With Two Different shRNAs.

Gene	shRNA	CI_{low}	CI_{high}	Log2 FC	*p* value
Ankrd34b	**Diras2_1**	**1.97**	**2.42**	**2.19**	**<1.00E-08**
	Diras2_2	**1.55**	**1.99**	**1.77**	**<1.00E-08**
Calcr	**Diras2_1**	**1.61**	**2.54**	**2.07**	**1.70E-07**
	Diras2_2	**0.90**	**1.84**	**1.37**	**1.99E-05**
Clasp2	**Diras2_1**	**1.49**	**2.08**	**1.79**	**<1.00E-08**
	Diras2_2	**1.61**	**2.20**	**1.91**	**<1.00E-08**
Clns1a	**Diras2_1**	**–1.42**	**–0.61**	**–1.02**	**9.53E-05**
	Diras2_2	**–2.61**	**–1.80**	**–2.21**	**1.00E-08**
Cpne8	**Diras2_1**	**–1.90**	**–0.96**	**–1.43**	**1.43E-05**
	Diras2_2	**–2.95**	**–2.01**	**–2.48**	**2.00E-08**
Ctdsp2	**Diras2_1**	**–0.84**	**–0.30**	**–0.57**	**5.18E-04**
	Diras2_2	**–2.15**	**–1.60**	**–1.88**	**<1.00E-08**
Eif2c2	**Diras2_1**	**1.47**	**2.09**	**1.78**	**<1.00E-08**
	Diras2_2	**1.64**	**2.26**	**1.95**	**<1.00E-08**
Epm2a	**Diras2_1**	**0.42**	**1.18**	**0.80**	**4.81E-04**
	Diras2_2	**0.63**	**1.39**	**1.01**	**5.50E-05**
Fktn	**Diras2_1**	**1.04**	**1.84**	**1.44**	**1.93E-06**
	Diras2_2	**1.61**	**2.41**	**2.01**	**3.00E-08**
Grb10	**Diras2_1**	**1.01**	**1.88**	**1.45**	**4.93E-06**
	Diras2_2	**1.52**	**2.39**	**1.95**	**1.40E-07**
Grin2a	**Diras2_1**	**0.52**	**1.34**	**0.93**	**2.58E-04**
	Diras2_2	**0.71**	**1.53**	**1.12**	**4.23E-05**
Ipo4	**Diras2_1**	**0.45**	**1.12**	**0.79**	**1.89E-04**
	Diras2_2	**0.76**	**1.43**	**1.09**	**6.44E-06**
Kcna3	**Diras2_1**	**0.93**	**1.58**	**1.26**	**8.40E-07**
	Diras2_2	**0.62**	**1.27**	**0.95**	**2.05E-05**
Kcnh1	**Diras2_1**	**0.72**	**1.83**	**1.27**	**2.29E-04**
	Diras2_2	**0.90**	**2.02**	**1.46**	**6.27E-05**
Kcnj3	**Diras2_1**	**1.08**	**1.55**	**1.31**	**<1.00E-08**
	Diras2_2	**0.71**	**1.17**	**0.94**	**4.80E-07**
Kdm3b	**Diras2_1**	**–1.48**	**–0.83**	**–1.16**	**2.12E-06**
	Diras2_2	**–2.39**	**–1.75**	**–2.07**	**<1.00E-08**
Lnp	**Diras2_1**	**1.16**	**1.60**	**1.38**	**<1.00E-08**
	Diras2_2	**1.13**	**1.58**	**1.36**	**<1.00E-08**
Lonrf2	**Diras2_1**	**1.09**	**1.62**	**1.36**	**3.00E-08**
	Diras2_2	**1.51**	**2.03**	**1.77**	**<1.00E-08**
Map3k2	**Diras2_1**	**0.55**	**0.83**	**0.69**	**4.00E-08**
	Diras2_2	**0.65**	**0.93**	**0.79**	**<1.00E-08**
Mettl9	**Diras2_1**	**–1.19**	**–0.45**	**–0.82**	**2.86E-04**
	Diras2_2	**–2.65**	**–1.91**	**–2.28**	**<1.00E-08**
Mfsd11	**Diras2_1**	**–1.71**	**–1.32**	**–1.52**	**<1.00E-08**
	Diras2_2	**–3.18**	**–2.78**	**–2.98**	**<1.00E-08**
Mpp5	**Diras2_1**	**0.52**	**1.43**	**0.97**	**4.11E-04**
	Diras2_2	**1.22**	**2.12**	**1.67**	**1.59E-06**
Purb	**Diras2_1**	**1.53**	**2.22**	**1.88**	**1.00E-08**
	Diras2_2	**1.03**	**1.72**	**1.37**	**6.50E-07**
Rgs17	**Diras2_1**	**1.42**	**2.23**	**1.83**	**1.30E-07**
	Diras2_2	**1.23**	**2.03**	**1.63**	**5.30E-07**
Rrm2	**Diras2_1**	**1.50**	**2.67**	**2.09**	**2.30E-06**
	Diras2_2	**2.44**	**3.61**	**3.03**	**3.00E-08**
Samd12	**Diras2_1**	**–1.13**	**–0.42**	**–0.77**	**3.85E-04**
	Diras2_2	**–2.71**	**–1.99**	**–2.35**	**<1.00E-08**
Setd7	**Diras2_1**	**1.84**	**2.62**	**2.23**	**<1.00E-08**
	Diras2_2	**3.00**	**3.79**	**3.39**	**<1.00E-08**
Tbc1d14	**Diras2_1**	**1.43**	**2.17**	**1.80**	**5.00E-08**
	Diras2_2	**2.07**	**2.81**	**2.44**	**<1.00E-08**
Tpi1	**Diras2_1**	**1.10**	**1.48**	**1.29**	**<1.00E-08**
	Diras2_2	**1.19**	**1.57**	**1.38**	**<1.00E-08**
Tppp	**Diras2_1**	**0.86**	**2.30**	**1.58**	**3.36E-04**
	Diras2_2	**1.09**	**2.53**	**1.81**	**9.74E-05**
Ubqln1	**Diras2_1**	**–1.20**	**–0.46**	**–0.83**	**2.83E-04**
	Diras2_2	**–2.73**	**–1.99**	**–2.36**	**<1.00E-08**
Unc80	**Diras2_1**	**0.79**	**1.78**	**1.28**	**7.08E-05**
	Diras2_2	**1.81**	**2.80**	**2.31**	**9.00E-08**
Usp8	**Diras2_1**	**–0.89**	**–0.44**	**–0.66**	**1.65E-05**
	Diras2_2	**–2.11**	**–1.67**	**–1.89**	**<1.00E-08**
Alg11	Diras2_1	0.13	1.26	0.70	0.01913
	Diras2_2	0.72	1.85	1.28	2.42E-04
Cdkn2aipnl	Diras2_1	0.39	1.44	0.92	0.00228
	Diras2_2	0.88	1.94	1.41	5.31E-05
Chrna7	Diras2_1	−0.86	−0.07	−0.47	0.02387
	Diras2_2	−3.15	−2.36	−2.75	<1.00E-08
Cntfr	Diras2_1	−0.71	−0.10	−0.41	0.01231
	Diras2_2	−2.90	−2.29	−2.59	<1.00E-08
Cntnap5a	Diras2_1	0.50	1.31	0.90	2.96E-04
	Diras2_2	0.22	1.03	0.63	0.00512
Epha3	Diras2_1	−1.22	−0.42	−0.82	6.43E-04
	Diras2_2	−2.69	−1.89	−2.29	<1.00E-08
Gnal	Diras2_1	0.31	2.40	1.36	0.01450
	Diras2_2	1.46	3.55	2.51	1.48E-04
Guk1	Diras2_1	−0.91	−0.10	−0.51	0.01774
	Diras2_2	−3.01	−2.20	−2.61	<1.00E-08
Lin7c	Diras2_1	−1.21	−0.29	−0.75	0.00363
	Diras2_2	−2.28	−1.36	−1.82	7.30E-07
Nacc1	Diras2_1	−1.30	−0.21	−0.76	0.01027
	Diras2_2	−2.42	−1.33	−1.87	3.62E-06
Nudt3	Diras2_1	0.38	1.16	0.77	0.00083
	Diras2_2	0.76	1.54	1.15	1.91E-05
Ppp1r9a	Diras2_1	0.17	0.91	0.54	0.00749
	Diras2_2	0.67	1.41	1.04	3.28E-05
Pxk	Diras2_1	−0.48	−0.11	−0.29	0.00475
	Diras2_2	−1.92	−1.55	−1.73	<1.00E-08
Rab3d	Diras2_1	0.28	1.27	0.77	0.00488
	Diras2_2	0.94	1.93	1.43	2.42E-05
Rictor	Diras2_1	0.14	0.46	0.30	0.00144
	Diras2_2	0.70	1.02	0.86	2.00E-08
Serinc5	Diras2_1	0.15	1.99	1.07	0.02602
	Diras2_2	0.70	2.54	1.62	0.00203
Siah3	Diras2_1	−1.29	−0.04	−0.66	0.03810
	Diras2_2	−3.94	−2.70	−3.32	2.00E-08
Slc30a9	Diras2_1	−0.97	−0.21	−0.59	0.00501
	Diras2_2	−2.80	−2.05	−2.42	<1.00E-08

(continued)

Table 1. (continued)

(continued)

Table 1. (continued)

Gene	shRNA	CI_{low}	CI_{high}	Log2 FC	*p* value
Syt17	Diras2_1	−2.58	−0.83	−1.71	9.33E-04
	Diras2_2	−3.07	−1.32	−2.20	9.78E-05
Trak2	Diras2_1	0.26	1.35	0.81	0.00701
	Diras2_2	0.87	1.96	1.41	7.34E-05
Trappc9	Diras2_1	−0.52	−0.03	−0.28	0.03156
	Diras2_2	−2.47	−1.97	−2.22	<1.00E-08
Trp53inp1	Diras2_1	0.29	1.10	0.69	0.00236
	Diras2_2	1.21	2.01	1.61	6.10E-07

Note. The genes that show significance after Bonferroni correction for multiple testing (significant $p = .00056$) for both shRNAs are bold. Print CI = 95%, log2 FC = log2 fold change compared with negative control (i.e., scrambled shRNA). qPCR = quantitative real-time PCR; shRNA = short hairpin RNA.

Gene-Based Association and Gene-Set Analysis

To test whether the 33 genes that were confirmed to be differentially expressed upon *Diras2* downregulation are associated with ADHD, we investigated the most recent ADHD GWAS of the Psychiatric Genomics Consortium (Demontis et al., 2017) for gene-based association of these 33 genes. Of the analyzed 32 genes (*TPI1* could not be annotated and was therefore removed from the analysis), seven genes (LONRF2, *MAP3K2, KCNJ3, TBC1D14, EIF2C2, UBQLN1*, and *IPO4*) demonstrated a nominal (i.e., before Bonferroni correction) gene-wise enrichment in ADHD. After Bonferroni correction, only *UBQLN1* remained significant (Table 2). Importantly, when analyzing the entire gene set of 32 genes, we found significant enrichment ($\beta = .341$, $SE = 0.153$, $p = .013$) of this gene set in ADHD patients.

Discussion

In this study, we aimed to investigate the molecular function of the ADHD-associated gene *DIRAS2*. We found that shRNA-mediated downregulation of *Diras2* in murine hippocampal primary cells changed the expression of more than 1,600 genes, which were associated with different GO pathways and coregulated gene modules.

The observed upregulation of genes involved in cell division and cell cycle indicates a role of *Diras2* in brain development. Indeed, among the genes whose expressional changes have been validated successfully by qPCR, several play a role in brain development. *Eif2c2*, also known as *Argonaut2* (*Ago2*) is a component of the RNA interference (RNAi) machinery. This gene, that is upregulated after *Diras2* knockdown, is crucial for developmental control and stem cell maintenance (Carmell, Xuan, Zhang, & Hannon, 2002) further corroborating a role for *Diras2* in brain development. It is conceivable that *Eif2c2* is upregulated as a consequence of shRNA-mediated activation of the RNA interference machinery. However, as a scrambled shRNA was used as a control, it appears more likely that the upregulation of *Eif2c2* expression is specific to the shRNAs targeting *Diras2* and, therefore, is caused by *Diras2* downregulation.

We were able to confirm several other differentially expressed genes involved in brain development that were confirmed by qPCR: *Clasp2* (cytoplasmic linker associated protein 2) plays a role in axon guidance (Lee et al., 2004) and mitotic fidelity (Pereira et al., 2006) both essential for brain development. *Ctdsp2* is involved in neuronal differentiation (Dill, Linder, Fehr, & Fischer, 2012) and in the suppression of gene expression in neuronal stem cells (Yeo et al., 2005). *Kcnh1* codes for a voltage-gated potassium channel (Kv10.1) that has been suggested to be involved in cognitive development (Cázares-Ordoñez & Pardo, 2017). The gene *Mpp5* is critical for proper cortical development by interacting with the mammalian target of rapamycin (mTOR) pathway (S. Kim et al., 2010), which by itself has been shown to be important for cortical development, but also to contribute to neurodevelopmental disorders (Takei & Nawa, 2014). Interestingly, *Rictor*, a gene coding for a scaffolding protein of one of the mTOR complexes (i.e., mTORC2) was also found to be differentially regulated by the Diras2_2 shRNA, though not by the Diras2_1 shRNA. Moreover, the differentially expressed genes *Fktn* (Foltz et al., 2016), *Rrm2* (He et al., 2017), and *Ubqln1* (Wu et al., 2002) have been shown to interact with the mTOR pathway. In fact, *Mtor* was also upregulated in the array (data not shown). Thus, potentially Di-Ras2 may be affecting brain development by interacting with the mTOR pathway. Of note, it has previously been shown that Di-Ras2 interacts with the mTOR pathway to control autophagy (Sutton et al., 2018).

Neurabin—a regulatory subunit of protein phosphatase 1 that is encoded by the *Ppp1r9a* gene (only significantly altered by shRNA Diras2_2)—is concentrated at the growth cone of neurons during their development (Nakanishi et al., 1997) and is known to regulate cell morphology (Oliver et al., 2002). Also, it is enriched in dendritic spines and seems to be involved in the regulation of spine morphology and their maturation (Hu, Huang, Roadcap, Shenolikar, & Xia, 2006). Investigating spine maturation and morphology after *Diras2* knockdown might lead to new insights into the role of this gene in regulating those important processes.

Expression of *Diras2* was shown to increase during brain development (Grünewald et al., 2018) providing further support to the assumption that it plays a critical role during this process. Therefore, proper regulation of *Diras2* expression during adolescence might be crucial for the control of cell division and the cell cycle in the maturing brain. As *Diras2* expression is predominantly found in glutamatergic cells in the cerebral cortex, hippocampus, and basolateral nucleus of the amygdala (Grünewald et al., 2018), it might be of particular importance for the development of

Table 2. Gene-Wise Association of 32 Genes Differentially Expressed Upon *Diras2* Downregulation With ADHD.

Gene symbol	Entrez ID	Chr	Start	n_{SNPs}	n_{Param}	*Z* value	*p* value	$p_{Bonferroni}$
KCNA3	3,738	1	111196182	37	6	−1.108	.866	1
KCNH1	3,756	1	210851657	1,389	75	0.263	.396	1
RRM2	6,241	2	10262695	12	3	0.234	.407	1
LONRF2	164,832	2	100889753	165	9	2.025	**.021**	0.685
MAP3K2	10,746	2	128056245	84	12	1.819	**.034**	1
KCNJ3	3,760	2	155555093	441	49	2.508	**.006**	0.194
LNPK	80,856	2	176790410	176	23	0.602	.274	1
CALCRL	10,203	2	188206690	230	20	1.133	129	1
UNC80	285,175	2	210636717	378	22	0.797	.213	1
CLASP2	23,122	3	33537737	288	19	1.060	145	1
TBC1D14	57,533	4	6911171	421	21	2.558	**.005**	0.168
SETD7	80,854	4	140427192	84	13	0.441	.330	1
TPPP	11,076	5	659977	52	4	−0.111	.544	1
ANKRD34B	340,120	5	79852574	35	8	1.190	.117	1
KDM3B	51,780	5	137688285	187	22	1.280	.100	1
EPM2A	7,957	6	145946440	261	12	0.312	.377	1
RGS17	26,575	6	153332026	391	20	1.484	.069	1
PURB	5,814	7	44915892	9	4	−0.235	.593	1
GRB10	2,887	7	50657760	622	29	0.055	.478	1
SAMD12	401,474	8	119201694	1,081	67	−0.163	.565	1
EIF2C2	27,161	8	141541264	279	29	2.873	**.002**	0.065
UBQLN1	29,979	9	86274878	123	11	3.377	**.000**	**0.012**
FKTN	2,218	9	108320411	152	20	−0.299	.618	1
CLNS1A	1,207	11	77327196	37	6	0.443	.329	1
CPNE8	144,402	12	39046002	589	23	0.349	.363	1
CTDSP2	10,106	12	58213710	26	4	0.483	.315	1
IPO4	79,711	14	24649425	15	5	2.054	**.020**	0.640
MPP5	64,398	14	67708012	295	12	−0.115	.546	1
USP8	9,101	15	50716579	235	18	0.772	.220	1
GRIN2A	2,903	16	9847265	1,700	50	0.780	.218	1
METTL9	51,108	16	21608543	55	11	−1.017	.845	1
MFSD11	79,157	17	74732647	21	8	0.278	.391	1

Note. Shown are N_{SNPs}, N_{Param}, the *Z* value, the raw *p* value, and the *p* value after Bonferrroni correction. Significant associations ($p \leq .05$) are shown in bold. N_{SNPs} = number of included SNPs in genes; N_{Param} = number of relevant parameters used in the model; SNP = single-nucleotide polymorphism.

glutamatergic circuits in these regions. In fact, several genes involved in glutamatergic signaling were affected by *Diras2* downregulation, including *Grin2a* (which was also validated by qPCR), *Grin3a, Grm5, Homer2, Nlgn2, Nrxn1*. Furthermore, this is supported by the significant GO-term enrichment for "glutamate metabolic process" in the analysis for differentially expressed genes as well as "regulation of glutamate receptor signaling" in the WGCNA analysis.

As ADHD is a neurodevelopmental disorder, our finding that *DIRAS2* may be affecting molecular pathways involved in neural development do support our hypothesis that this gene may be a candidate gene for ADHD. This assumption is further supported by our finding that the set of genes that showed differential expression upon downregulation of *Diras2* showed significant enrichment in ADHD patients. Moreover, several studies have indicated that glutamatergic signaling (Moretto, Murru, Martano, Sassone, & Passafaro, 2018) and disturbed development of dendritic spines may be involved in the symptomatology of ADHD and in the mode of action of methylphenidate (Y. Kim et al., 2009; Zehle, Bock, Jezierski, Gruss, & Braun, 2007), the most commonly prescribed ADHD treatment, further supporting a potential role of *DIRAS2* in the development of ADHD.

In addition to the association with neural development, GO-term analysis showed significant enrichment in several other pathways. The strongest enrichment for genes upregulated upon *Diras2* knockdown is seen for "negative regulation of signal transduction by p53 class mediator." The protein p53 is one of the best studied tumor suppressor molecules (Levine & Oren, 2009). Of note, a recent report showed downregulation of *Diras2* (and also *Diras1*) in ovarian cancer cells and reduction of cancer cell growth

upon reexpression of *Diras1* or *Diras2* (Sutton et al., 2018). Sutton et al. (2018) suggested that Di-Ras2, similar to Di-Ras3 (aka ARHI or NOEY2; Y. Yu et al., 1999), may act as a tumor suppressor through autophagy-mediated cell death. Importantly, we also found enrichment of the "autophagy" GO-term in both up- and downregulated gene sets. Interestingly, we did not observe changes in the expression of *Trp53* (the murine gene coding for p53) by *Diras2* knockdown (data not shown), suggesting that Di-Ras2 does not directly affect p53.

For genes downregulated by *Diras2* knockdown, the strongest enrichment is seen for "positive regulation of GTPase activity." This is particularly striking as Di-Ras2 has been suggested to have little to no GTPase activity (Kontani et al., 2002). However, to the best of our knowledge, no other study so far has investigated the GTPase activity of Di-Ras2.

Of note, we could observe a strong enrichment in pathways involved in protein synthesis, protein transport, and protein modification. Although it is possible that Di-Ras2, or the lack thereof, has a direct effect on these pathways, this change is more parsimoniously explained by the massive change in protein composition caused by *Diras2* downregulation. Likewise, the observed enrichment in pathways involved in DNA and RNA replication, transport, and stability could be due to a genuine effect of Di-Ras2 on these pathways or due to a consequence in overall gene expression–level changes. Thus, at the current stage, it remains unclear if all of the observed alterations and gene-network level changes are directly or indirectly affected by *Diras2* downregulation and warrant further investigation.

As described above, the ADHD risk allele of *Diras2* results in increased expression of this gene. Therefore, overexpression of *Diras2* would more directly model the effect of the risk allele. However, as the rates of overexpression can vary strongly between experiments and normally exceed those caused by genetic variants, shRNA-mediated knockdown yields better controlled and more consistent conditions. Moreover, investigating the effects of *Diras2* downregulation allowed us to identify the genes/molecular pathways dependent on *Diras2* expression, bringing us much closer to understand the physiological role of this gene than overexpression would. Therefore, we decided to investigate the effects of *Diras2* expression changes using a knockdown strategy.

Further investigations, for example, using neuronal cultures derived from induced pluripotent stem cells (including those from risk variant carriers) or genome-wide expression data showing the impact of *DIRAS2* on the identified genes and pathways will be needed to replicate and generalize our findings. Also, phenotypic and functional studies in cell and animal models with altered *Diras2* expression are necessary to gather further knowledge about the functional role of this gene.

Taken together, our findings suggest a role of *DIRAS2* in a variety of pathways involved in neural development, mitochondric function, dendritic spine maturation, and executive functioning. Although we do not provide direct evidence for the involvement of *DIRAS2* in ADHD, our findings support the hypothesis that *DIRAS2* might be critically involved in the pathophysiology of this disorder. Further investigations of this ADHD candidate gene might lead to new insights into the development of this disorder and could help finding new targets for ADHD treatment.

Authors' Note

Florian Freudenberg and Andreas Reif share last authorship.

Declaration of Conflicting Interests

The author(s) declared the following potential conflicts of interest with respect to the research, authorship, and/or publication of this article: L.G., A.G.C., C.J.S., F.F., H.W., and C.S. declare to have no conflict of interest. A.R. has received speaker's honoraria and grant support from Medice.

Funding

The author(s) disclosed receipt of the following financial support for the research, authorship, and/or publication of this article: A.R. and his team are supported by funding from the European Community's Seventh Framework Programme (FP7/2007-2013) under grant agreements: 602805 (Aggressotype) and from the European Community's Horizon 2020 program (H2020/2014-2020) under grant agreements: 643051 (MiND) and 667302 (CoCA). In addition, this work was supported by the ECNP for the Research Network "ADHD across the Lifespan." This study has been supported in part by the Alexander von Humboldt Foundation (Feodor Lynen Return Fellowship to F.F.).

Supplemental Material

Supplemental material for this article is available online.

References

Alexa, A., Rahnenfuhrer, J., & Lengauer, T. (2006). Improved scoring of functional groups from gene expression data by decorrelating GO graph structure. *Bioinformatics*, *22*, 1600-1607. doi:10.1093/bioinformatics/btl140

Asherson, P., Zhou, K., Anney, R. J. L., Franke, B., Buitelaar, J., Ebstein, R., . . . Faraone, S. V. (2008). A high-density SNP linkage scan with 142 combined subtype ADHD sib pairs identifies linkage regions on chromosomes 9 and 16. *Molecular Psychiatry*, *13*, 514-521. doi:10.1038/sj.mp.4002140

Auton, A., Abecasis, G. R., Altshuler, D. M., Durbin, R. M., Bentley, D. R., Chakravarti, A., . . . Lu, Y. (2015). A global reference for human genetic variation. *Nature*, *526*, 68-74. doi:10.1038/nature15393

Brummelkamp, T. R., Bernards, R., & Agami, R. (2002). A system for stable expression of short interfering RNAs in mammalian cells. *Science*, *296*, 550-553. doi:10.1126/science.1068999

Candemir, E., Kollert, L., Weißflog, L., Geis, M., Müller, A., Post, A. M., . . . Freudenberg, F. (2016). Interaction of NOS1AP with the NOS-I PDZ domain: Implications for schizophrenia-related alterations in dendritic morphology. *European Neuropsychopharmacology*, *26*, 741-755. doi:10.1016/j.euroneuro.2016.01.008

Carmell, M. A., Xuan, Z., Zhang, M. Q., & Hannon, G. J. (2002). The Argonaute family: Tentacles that reach into RNAi, developmental control, stem cell maintenance, and tumorigenesis. *Genes & Development*, *16*, 2733-2742. doi:10.1101/gad.1026102

Cázares-Ordoñez, V., & Pardo, L. A. (2017). Kv10.1 potassium channel: From the brain to the tumors. *Biochemistry and Cell Biology*, *95*, 531-536. doi:10.1139/bcb-2017-0062

Chiocchetti, A. G., Haslinger, D., Stein, J. L., de la Torre-Ubieta, L., Cocchi, E., Rothämel, T., . . . Freitag, C. M. (2016). Transcriptomic signatures of neuronal differentiation and their association with risk genes for autism spectrum and related neuropsychiatric disorders. *Translational Psychiatry*, *6*(8), e864. doi:10.1038/tp.2016.119

de Leeuw, C. A., Mooij, J. M., Heskes, T., & Posthuma, D. (2015). MAGMA: Generalized gene-set analysis of GWAS data. *PLoS Computational Biology*, *11*(4), e1004219. doi:10.1371/journal.pcbi.1004219

Demontis, D., Walters, R. K., Martin, J., Mattheisen, M., Als, T. D., Agerbo, E., . . . Neale, B. M. (2018) Discovery of the first genome-wide significant risk loci for attention deficit/hyperactivity disorder. *Nature Genetics*. doi: 10.1038/s41588-018-0269-7.

Dill, H., Linder, B., Fehr, A., & Fischer, U. (2012). Intronic miR-26b controls neuronal differentiation by repressing its host transcript, ctdsp2. *Genes & Development*, *26*, 25-30. doi:10.1101/gad.177774.111

Epstein, J. N., & Loren, R. E. A. (2013). Changes in the definition of ADHD in DSM-5: Subtle but important. *Neuropsychiatry*, *3*, 455-458. doi:10.2217/npy.13.59

Faraone, S. V., Asherson, P., Banaschewski, T., Biederman, J., Buitelaar, J. K., Ramos-Quiroga, J. A., . . . Franke, B. (2015). Attention-deficit/hyperactivity disorder. *Nature Reviews Disease Primers*, *1*, 15020. doi:10.1038/nrdp.2015.20

Faraone, S. V., Perlis, R. H., Doyle, A. E., Smoller, J. W., Goralnick, J. J., Holmgren, M. A., & Sklar, P. (2005). Molecular genetics of attention-deficit/hyperactivity disorder. *Biological Psychiatry*, *57*, 1313-1323. doi:10.1016/j.biopsych.2004.11.024

Foltz, S. J., Luan, J., Call, J. A., Patel, A., Peissig, K. B., Fortunato, M. J., & Beedle, A. M. (2016). Four-week rapamycin treatment improves muscular dystrophy in a fukutin-deficient mouse model of dystroglycanopathy. *Skeletal Muscle*, *6*, 20. doi:10.1186/s13395-016-0091-9

Grünewald, L., Becker, N., Camphausen, A., O'Leary, A., Lesch, K.-P., Freudenberg, F., & Reif, A. (2018). Expression of the ADHD candidate gene Diras2 in the brain. *Journal of Neural Transmission*, *125*, 913-923. doi:10.1007/s00702-018-1867-3

Grünewald, L., Landaas, E. T., Geissler, J., Weber, H., Quast, C., Röh, S., . . . Reif, A. (2016). Functional impact of an ADHD-associated DIRAS2 promoter polymorphism. *Neuropsychopharmacology*, *41*, 3025-3031. doi:10.1038/npp.2016.113

Haslinger, D., Waltes, R., Yousaf, A., Lindlar, S., Schneider, I., Lim, C. K., . . . Chiocchetti, A. G. (2018). Loss of the Chr16p11.2 ASD candidate gene QPRT leads to aberrant neuronal differentiation in the SH-SY5Y neuronal cell model 06 biological sciences 0604 genetics. *Molecular Autism*, *9*, 1-17. doi:10.1186/s13229-018-0239-z

He, Z., Hu, X., Liu, W., Dorrance, A., Garzon, R., Houghton, P. J., & Shen, C. (2017). P53 suppresses ribonucleotide reductase via inhibiting mTORC1. *Oncotarget*, *8*, 41422-41431. doi:10.18632/oncotarget.17440

Hu, X. D., Huang, Q., Roadcap, D. W., Shenolikar, S. S., & Xia, H. (2006). Actin-associated neurabin-protein phosphatase-1 complex regulates hippocampal plasticity. *Journal of Neurochemistry*, *98*, 1841-1851. doi:10.1111/j.1471-4159.2006.04070.x

Kaech, S., & Banker, G. (2006). Culturing hippocampal neurons. *Nature Protocols*, *1*, 2406-2415. doi:10.1038/nprot.2006.356

Kim, S., Lehtinen, M. K., Sessa, A., Zappaterra, M. W., Cho, S.-H., Gonzalez, D., . . . Walsh, C. A. (2010). The apical complex couples cell fate and cell survival to cerebral cortical development. *Neuron*, *66*, 69-84. doi:10.1016/j.neuron.2010.03.019

Kim, Y., Teylan, M. A., Baron, M., Sands, A., Nairn, A. C., & Greengard, P. (2009). Methylphenidate-induced dendritic spine formation and DeltaFosB expression in nucleus accumbens. *Proceedings of the National Academy of Sciences of the United States of America*, *106*, 2915-2920. doi:10.1073/pnas.0813179106

Kontani, K., Tada, M., Ogawa, T., Okai, T., Saito, K., Araki, Y., & Katada, T. (2002). Di-Ras, a distinct subgroup of ras family GTPases with unique biochemical properties. *Journal of Biological Chemistry*, *277*, 41070-41078. doi:10.1074/jbc.M202150200

Lee, H., Engel, U., Rusch, J., Scherrer, S., Sheard, K., & Van Vactor, D. (2004). The microtubule plus end tracking protein Orbit/MAST/CLASP acts downstream of the tyrosine kinase Abl in mediating axon guidance. *Neuron*, *42*, 913-926. doi:10.1016/j.neuron.2004.05.020

Lesch, K.-P., Timmesfeld, N., Renner, T. J., Halperin, R., Röser, C., Nguyen, T. T., . . . Jacob, C. (2008). Molecular genetics of adult ADHD: Converging evidence from genome-wide association and extended pedigree linkage studies. *Journal of Neural Transmission*, *115*, 1573-1585. doi:10.1007/s00702-008-0119-3

Levine, A. J., & Oren, M. (2009). The first 30 years of p53: Growing ever more complex. *Nature Reviews Cancer*, *9*, 749-758. doi:10.1038/nrc2723

Martin, J., Walters, R. K., Demontis, D., Mattheisen, M., Lee, S. H., Robinson, E., . . . Neale, B. M. (2017). A genetic investigation of sex bias in the prevalence of attention deficit/hyperactivity disorder. *Biological Psychiatry*, *83*, 1044-1053. doi:10.1016/J.BIOPSYCH.2017.11.026

Matthews, M., Nigg, J. T., & Fair, D. A. (2014). Attention deficit hyperactivity disorder. *Current Topics in Behavioral Neurosciences*, *16*, 235-266. doi:10.1007/7854_2013_249

Moretto, E., Murru, L., Martano, G., Sassone, J., & Passafaro, M. (2018). Glutamatergic synapses in neurodevelopmental disorders. *Progress in Neuro-Psychopharmacology & Biological Psychiatry*, *84*, 328-342. doi:10.1016/J.PNPBP.2017.09.014

Nakanishi, H., Obaishi, H., Satoh, A., Wada, M., Mandai, K., Satoh, K., . . . Takai, Y. (1997). Neurabin: A novel neural tissue-specific actin filament-binding protein involved in neurite formation. *The Journal of Cell Biology*, *139*, 951-961.

Naughton, B. J., Han, D. D., & Gu, H. H. (2011). Fluorescence-based evaluation of shRNA efficacy. *Analytical Biochemistry*, *417*, 162-164. doi:10.1016/j.ab.2011.06.008

Neale, B. M., Medland, S. E., Ripke, S., Asherson, P., Franke, B., Lesch, K.-P., . . . Nelson, S. (2010). Meta-analysis of genome-wide association studies of attention-deficit/hyperactivity disorder. *Journal of the American Academy of Child and Adolescent Psychiatry*, *49*, 884-897. doi:10.1016/j.jaac.2010.06.008

Nigg, J., Nikolas, M., & Burt, S. A. (2010). Measured gene by environment interaction in relation to attention-deficit/hyperactivity disorder. *Journal of the American Academy of Child and Adolescent Psychiatry*, *49*, 863-873. doi:10.1016/j.jaac.2010.01.025

Oliver, C. J., Terry-Lorenzo, R. T., Elliott, E., Bloomer, W. A. C., Li, S., Brautigan, D. L., . . . Shenolikar, S. (2002). Targeting protein phosphatase 1 (PP1) to the actin cytoskeleton: The neurabin I/PP1 complex regulates cell morphology. *Molecular and Cellular Biology*, *22*, 4690-4701.

Pereira, A. L., Pereira, A. J., Maia, A. R. R., Drabek, K., Sayas, C. L., Hergert, P. J., . . . Maiato, H. (2006). Mammalian CLASP1 and CLASP2 cooperate to ensure mitotic fidelity by regulating spindle and kinetochore function. *Molecular Biology of the Cell*, *17*, 4526-4542. doi:10.1091/mbc.E06-07-0579

Reif, A., Nguyen, T. T., Weißflog, L., Jacob, C. P., Romanos, M., Renner, T. J., . . . Lesch, K.-P. (2011). DIRAS2 is associated with adult ADHD, related traits, and co-morbid disorders. *Neuropsychopharmacology*, *36*, 2318-2327. doi:10.1038/npp.2011.120

Romanos, M., Freitag, C., Jacob, C., Craig, D. W., Dempfle, A., Nguyen, T. T., . . . Lesch, K. P. (2008). Genome-wide linkage analysis of ADHD using high-density SNP arrays: Novel loci at 5q13.1 and 14q12. *Molecular Psychiatry*, *13*, 522-530. doi:10.1038/mp.2008.12

Smyth, G. K. (2004). Linear models and empirical Bayes methods for assessing differential expression in microarray experiments. *Statistical Applications in Genetics and Molecular Biology*, *3*(1), 3. doi:10.2202/1544-6115.1027

Sutton, M. N., Yang, H., Huang, G. Y., Fu, C., Pontikos, M., Wang, Y., . . . Bast, R. C. (2018). RAS-related GTPases DIRAS1 and DIRAS2 induce autophagic cancer cell death and are required for autophagy in murine ovarian cancer cells. *Autophagy*, *14*, 637-653. doi:10.1080/15548627.2018.1427022

Takei, N., & Nawa, H. (2014). mTOR signaling and its roles in normal and abnormal brain development. *Frontiers in Molecular Neuroscience*, *7*, 28. doi:10.3389/fnmol.2014.00028

Thapar, A., & Cooper, M. (2016). Attention deficit hyperactivity disorder. *The Lancet*, *387*, 1240-1250. doi:10.1016/S0140-6736(15)00238-X

Wu, S., Mikhailov, A., Kallo-Hosein, H., Hara, K., Yonezawa, K., & Avruch, J. (2002). Characterization of ubiquilin 1, an mTOR-interacting protein. *Biochimica et Biophysica Acta (BBA)—Molecular Cell Research*, *1542*(1–3), 41-56. doi:10.1016/S0167-4889(01)00164-1

Yeo, M., Lee, S. K., Lee, B., Ruiz, E. C., Pfaff, S. L., & Gill, G. N. (2005). Small CTD phosphatases function in silencing neuronal gene expression. *Science*, *307*, 596-600. doi:10.1126/science.1100801

Yu, J.-Y., DeRuiter, S. L., & Turner, D. L. (2002). RNA interference by expression of short-interfering RNAs and hairpin RNAs in mammalian cells. *Proceedings of the National Academy of Sciences of the United States of America*, *99*, 6047-6052. doi:10.1073/pnas.092143499

Yu, Y., Xu, F., Peng, H., Fang, X., Zhao, S., Li, Y., . . . Bast, R. C. (1999). NOEY2 (ARHI), an imprinted putative tumor suppressor gene in ovarian and breast carcinomas. *Proceedings of the National Academy of Sciences of the United States of America*, *96*, 214-219. doi:10.1073/pnas.96.1.214

Zehle, S., Bock, J., Jezierski, G., Gruss, M., & Braun, K. (2007). Methylphenidate treatment recovers stress-induced elevated dendritic spine densities in the rodent dorsal anterior cingulate cortex. *Developmental Neurobiology*, *67*, 1891-1900. doi:10.1002/dneu.20543

Author Biographies

Lena Grünewald, PhD, received her training in biology at the Universities of Karlsruhe and Würzburg. She completed her PhD at the University of Würzburg studying the genetics of ADHD. She now is the lab manager at the Laboratory of Translational Psychiatry, at the Department of Psychiatry, Psychosomatic Medicine and Psychotherapy of the University Hospital Frankfurt investigating the molecular mechanism of mental disorders.

Andreas G. Chiocchetti, PhD, is a geneticist who received his training at the University of Salzburg and the German Cancer Research Center. He is the head of the Molecular Genetics Laboratory at the Department of Child and Adolescent Psychiatry, Psychosomatic Medicine and Psychotherapy, University Hospital Frankfurt.

Heike Weber, PhD, is a bioinformatician investigating the genetics of mental disorders. She studied Biotechnology at the University of Kaiserslautern and did her PhD at the University of Ulm, and currently holds a shared postdoctoral appointment at the University Hospitals Frankfurt and Würzburg.

Claus-Jürgen Scholz, PhD, is a bioinformatician who returned—after a few years in molecular biological work in cancer research—to bioinformatics. He is interested in (epi-) genetics and transcriptomics with the focus on single-cell analyses.

Christoph Schartner, PhD, is a postdoctoral researcher at the University of California, San Francisco. He performed his PhD at the University of Würzburg investigating the molecular mechanisms of risk genes involved in mental disorders.

Florian Freudenberg, PhD, is the group leader of molecular psychiatry at the Department of Psychiatry, Psychosomatic Medicine and Psychotherapy of the University Hospital Frankfurt. He is working on the molecular mechanisms involved in affective and psychotic disorders. He received his training in biology at the University of Bremen and did his PhD at the University of Heidelberg.

Andreas Reif, MD, underwent medical training and specialization in psychiatry at the University Hospital of Würzburg, where he later became vice chair at the Department of Psychiatry, Psychosomatics and Psychotherapy. He is now chair of the Department of Psychiatry, Psychosomatic Medicine and Psychotherapy at the University Hospital Frankfurt.